

## Consistent spatial patterns in multiple trophic levels occur around artificial habitats

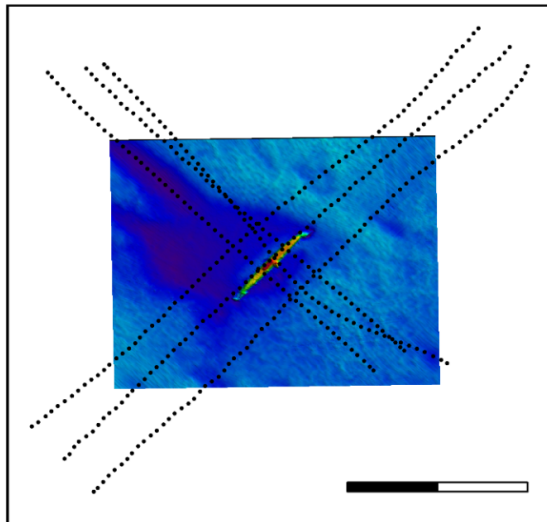
Avery B. Paxton\*, J. Christopher Taylor, C.H. Peterson, Stephen R. Fegley, Johanna H. Rosman

\*Corresponding author: avery.paxton@duke.edu

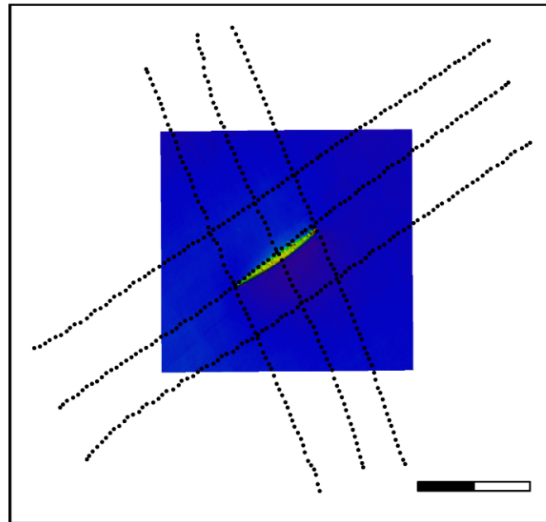
Marine Ecology Progress Series 611: 189–202 (2019)

### Supplement 1

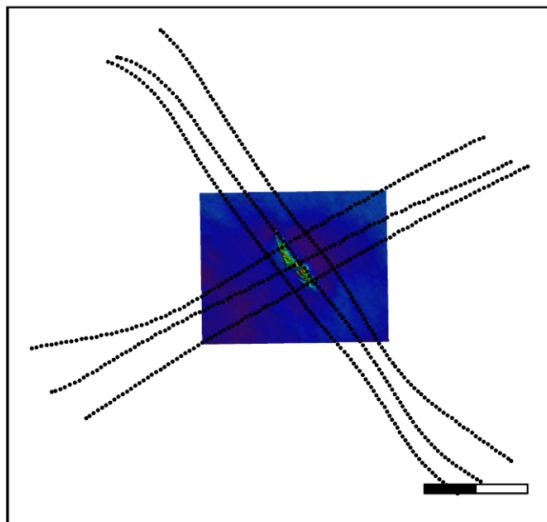
a) U-352 (2017-07-06)



c) USS *Tarpon* (2016-11-01)



b) USS *Schurz* (2017-07-12)



d) *W.E. Hutton* (2017-07-10)

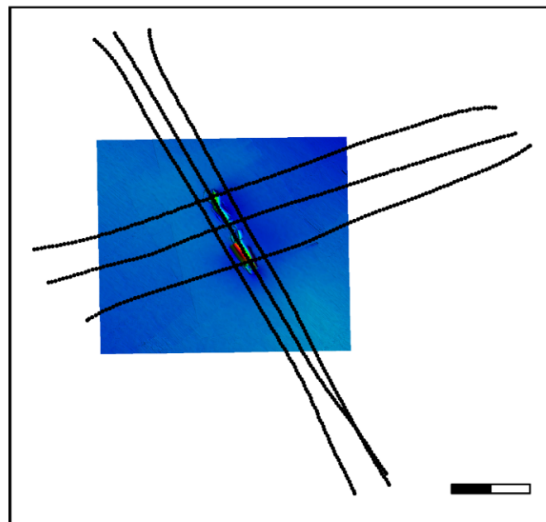


**Figure S1.** Bathymetric maps of four surveyed shipwrecks: a) U-352, b) USS *Schurz*, c) USS *Tarpon*, and d) *W.E. Hutton*. Warm colors are shallower depths; cool colors are deeper depths. Black dotted lines are survey paths. North is up. Each scale bar is a total of 100 m; the scale division occurs at 50 m. The date surveyed (yyyy-mm-dd) is displayed.

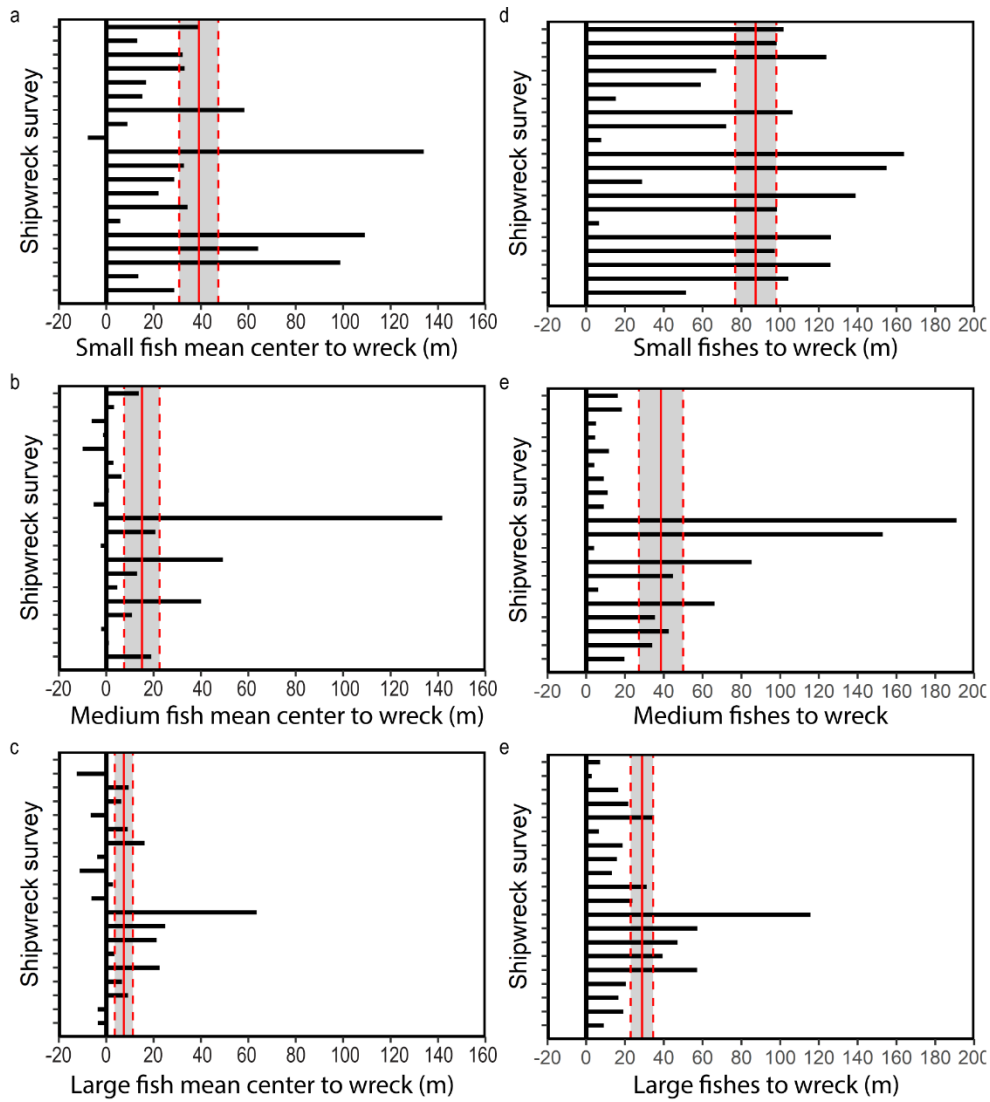


**Figure S2.** Distance of fishes from nearest shipwreck edges. a-c) Distance between the mean center of a) small fishes, b) medium fishes, and c) large fishes and the nearest shipwreck edge for each shipwreck survey. d-f) Mean distance of sample cells containing d) small fishes, e) medium fishes, and f) large fishes and the nearest shipwreck edge. Positive distances are outwards of shipwreck structures; negative distances are within shipwreck structures. Horizontal lines (black) represent individual surveys (N=20), and the sequence of surveys (Table S2) remains consistent among panels. Vertical lines are mean (solid red)  $\pm$  standard error (dashed red).

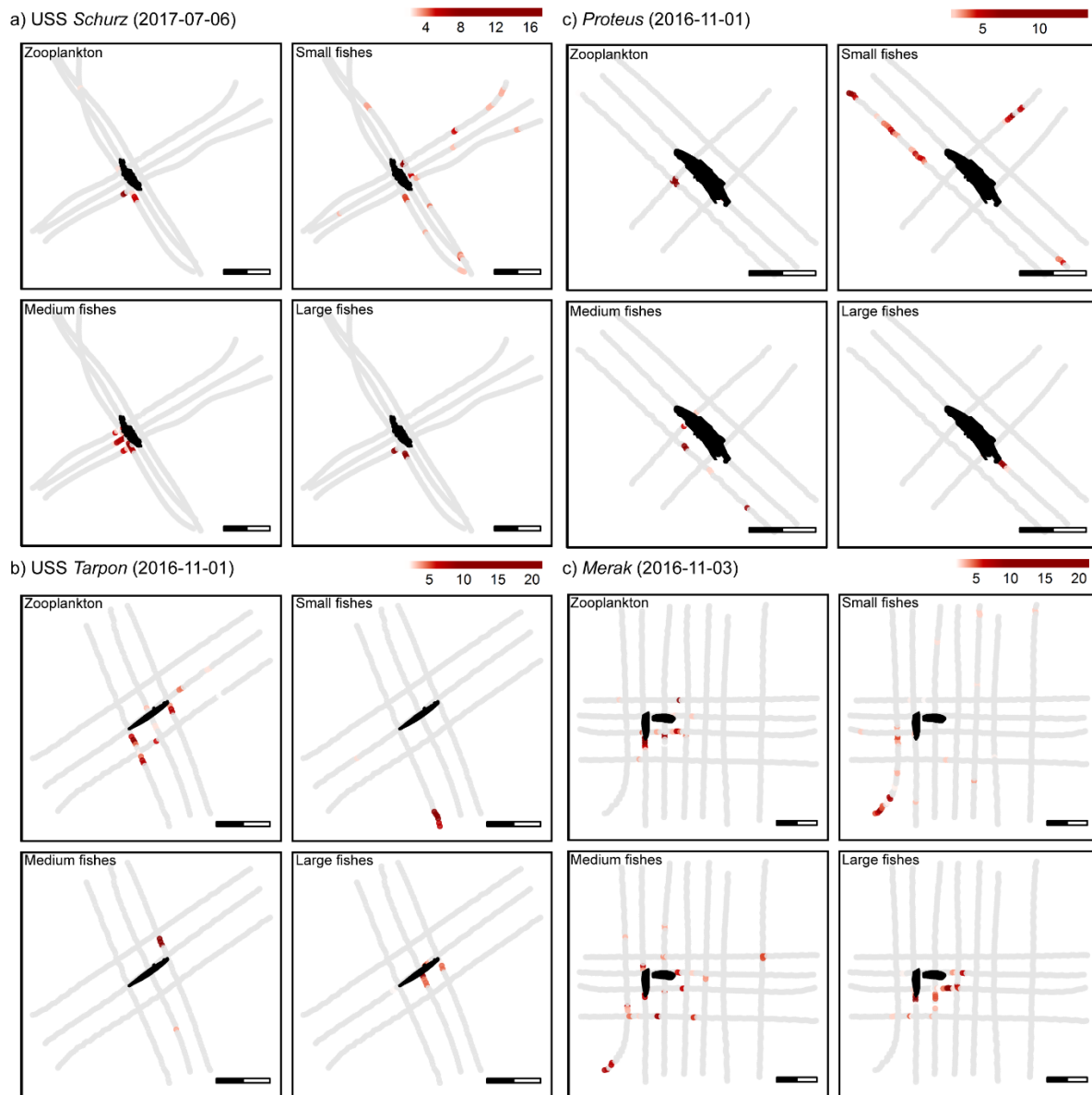


**Figure S3.** Spatial clusters of zooplankton, small fishes, medium fishes, and large fishes relative to each of four shipwrecks (black): a) USS *Schurz*, b) USS *Tarpon*, c) *Proteus*, and d) *Merak*. Colors correspond to the Getis-Ord  $G_i^*$  z-value, where darker red represents more pronounced areas of high density (hot-spots). Gray points are locations along the survey where data were obtained but the the Getis-Ord  $G_i^*$  z-value was not significant. North is up. Each scale bar is a total of 100 m; the scale division occurs at 50 m. The date surveyed (yyyy-mm-dd) is displayed.

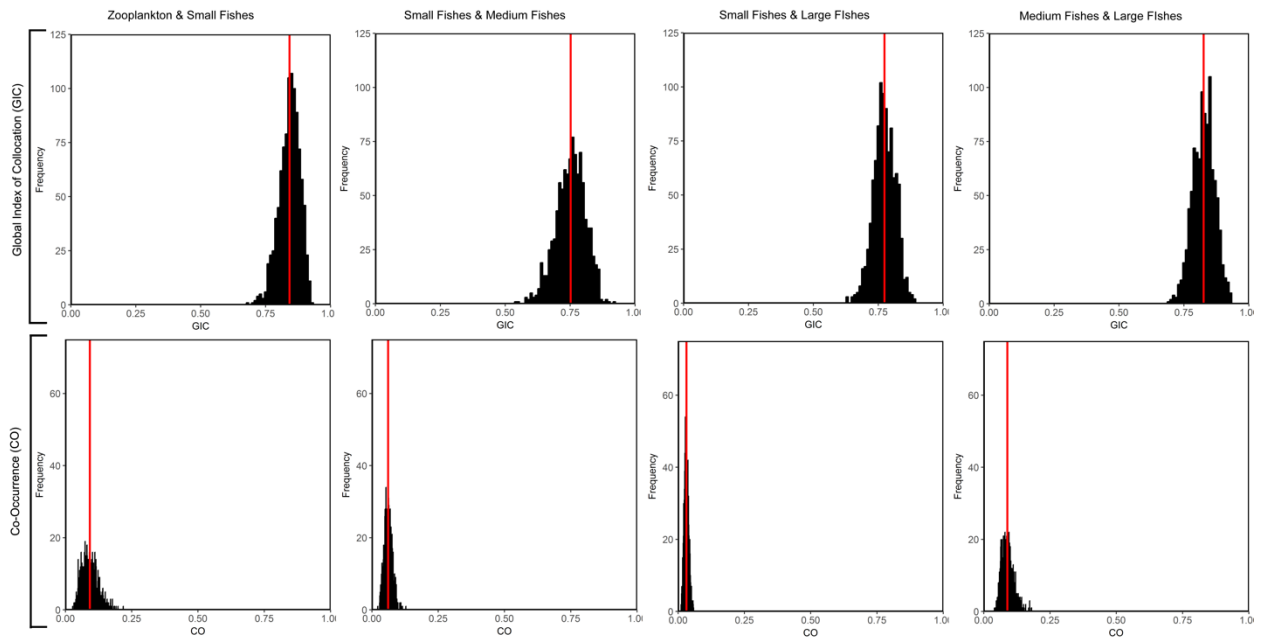


**Figure S4.** Bootstrapped metrics describing spatial relationships between pairs of organisms. Black bars represent the distribution from the 20 surveys following bootstrapping with 1,000 samples. Red vertical lines represent the mean across all twenty surveys. Columns correspond to organism pairs: zooplankton and small fishes, small fishes and medium fishes, small fishes and large fishes, and medium fishes and large fishes. Rows correspond to overlap metrics: global index of collocation (GIC) and co-occurrence (CO).

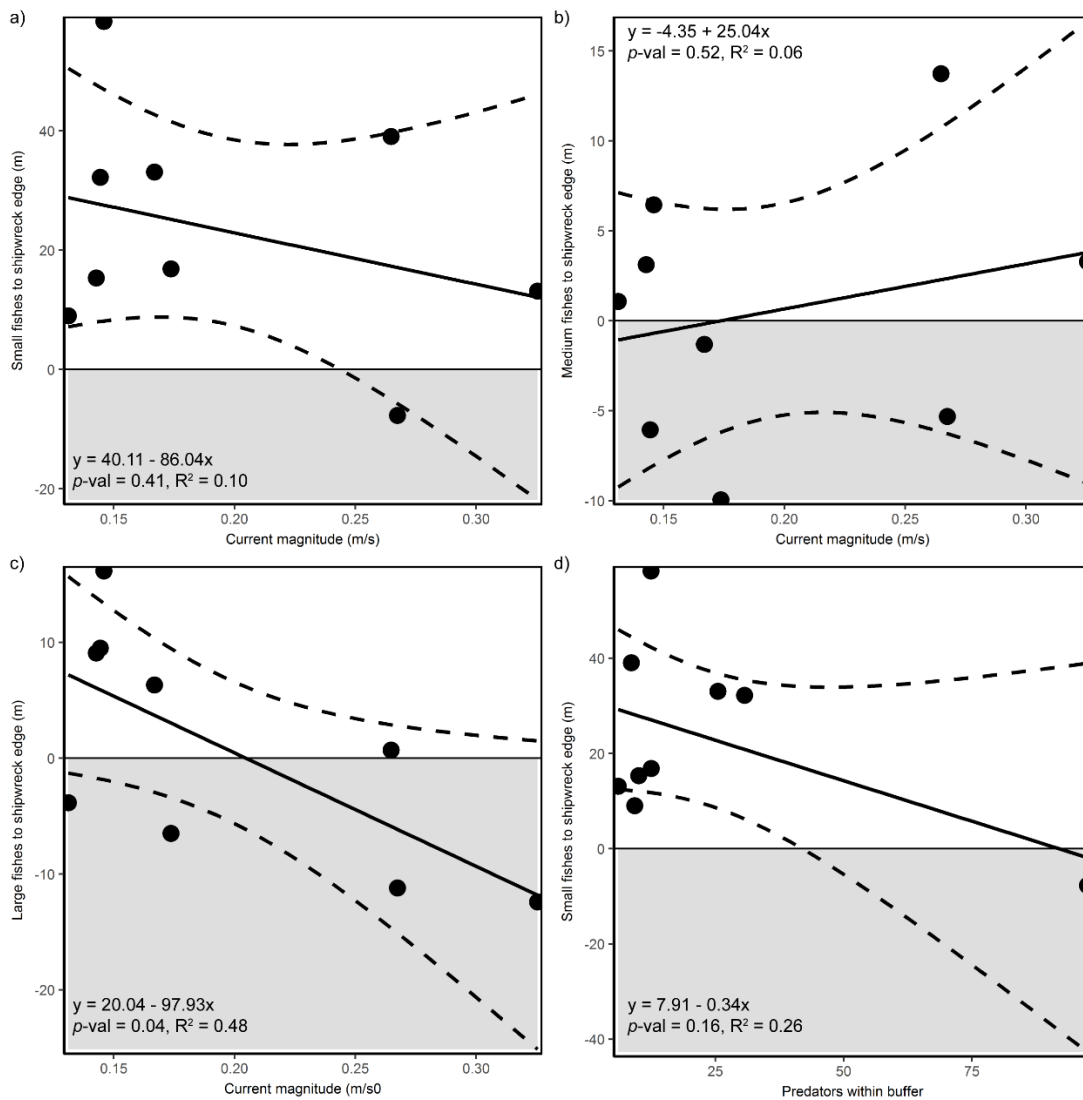


**Figure S5.** a-c) Relationships between current magnitude and distances of a) small fishes, b) medium fishes, and c) large fishes from shipwreck, d) Relationship between number of predators on shipwrecks and within 5 m outward of shipwrecks. Linear regression displayed as solid line. Dashed lines are standard error. Raw data are points. Shaded gray areas represent fishes directly above the shipwreck structure, whereas white areas represent fishes located outwards of the shipwreck structure.

**Table S1** Descriptions of fifteen shipwrecks surveyed. Shipwreck metrics include mean depth (mean dep), maximum depth (max dep), minimum depth (min dep), vertical relief (relief), area on wreckage on the seafloor (area), and perimeter of wreckage on the seafloor (perimeter). Width and length of the originally built ship and the sunken wreckage on the seafloor are provided. Bathymetry and transect lines for survey for several wrecks are displayed in Figure S1. Historical data for each shipwreck, such as date of sinking and original ship specifications, were provided by the NOAA *Monitor* National Marine Sanctuary.

Ship name	Ship type	Material	Built length [m]	Built width [m]	Date sunk	Sinking description	Mean dep [m]	Max dep [m]	Min dep [m]	Relief [m]	Area [m <sup>2</sup> ]	Perim [m]	Sunk width [m]	Sunk length [m]
<i>Ashkhabad</i>	Tanker	steel	122.2	15.9	1942	sunk by U-402	-17.7	-18.9	-13.4	5.4	2657.6	293.5	44.8	104.8
<i>Empire Thrush</i>	Steam Merchant	steel	120.5	16.8	1942	sunk by U-203	-20.6	-22.3	-19.3	3.1	32.6	27.0	5.9	24.0
<i>F.W. Abrams</i>	Tanker	steel	142.5	19.1	1942	sunk by mine	-25.0	-26.0	-21.1	4.9	3261.2	407.4	39.5	158.6
<i>HMS Senateur</i>	Trawler (converted to anti-submarine)	steel	58.6	9.5	1942	collision with USS <i>Semmes</i>	-18.7	-19.8	-15.8	4.0	858.5	164.8	23.3	62.0
<i>Duhamel HMT</i>	Trawler (converted to convoy escort)	steel	49.5	8.1	1942	sunk by U-140	-29.1	-29.6	-27.4	2.2	385.7	116.9	27.1	34.0
<i>Bedfordshire</i>	Cargo Ship	steel	101.7	14.6	1942	sunk by U-160	-59.6	-61.1	-56.1	5.0	2005.6	288.2	29.1	107.9
<i>Malchace</i>	Steam Merchant	steel	99.4	14.3	1918	sunk by U-140	-38.0	-43.5	-33.0	10.5	1485.4	257.3	47.5	87.1
<i>Merak</i>	Passenger / Freighter	steel	118.9	14.6	1918	collision with SS <i>Cushing</i>	-36.0	-38.0	-31.4	6.6	2335.2	320.0	31.2	121.0
<i>Proteus</i>	U-boat (VII C)	steel	67.1	6.1	1942	sunk by USS <i>Icarus</i>	-32.0	-34.1	-29.8	4.3	372.2	139.2	9.1	64.7
U-352	U-boat (VII C)	steel	67.1	6.1	1942	sunk by US Army Hudson aircraft	-33.1	-35.4	-30.8	4.6	283.2	141.7	7.4	68.2
U-701	U-boat (VII C)	steel	67.1	6.1	1942	sunk in storm	-66.9	-68.8	-64.6	4.2	558.0	115.7	16.2	45.7
USS <i>Monitor</i>	Ironclad	iron	52.7	12.6	1862	collision with SS <i>Florida</i>	-32.4	-33.3	-29.6	3.7	1111.1	226.3	22.1	81.9
USS <i>Schurz</i>	Gunboat	composite hull wood / steel	68.6	9.8	1918	intentionally sunk	-39.8	-42.2	-37.3	4.8	510.8	180.5	10.2	84.7
USS <i>Tarpon</i>	Submarine	steel	90.8	7.6	1957	sunk by U-701	-96.0	-98.6	-94.2	4.4	277.1	79.9	9.3	36.3
USS YP-389	Trawler (converted to patrol)	steel	31.2	6.7	1942									
<i>W.E. Hutton</i>	Tanker	steel	132.6	17.1	1942	sunk by U-124	-33.2	-37.1	-26.6	10.5	2293.8	353.5	25.3	141.2

**Table S2.** Descriptions of twenty surveys across fifteen shipwrecks. Survey number corresponds to the order from top to bottom of surveys in Figure S3. MBES resolution (res) indicates the resolution of multibeam bathymetry data used to delineate shipwrecks and establish transect lines. SBES and ADCP indicate whether these two instruments were active (X) or inactive (--). Area surveyed is the total area surveyed in m<sup>2</sup>.

Survey	Date	Shipwreck	MBES res (m)	SBES	ADCP	Area Surveyed (m <sup>2</sup> )
1	2016-11-01	HMT <i>Bedfordshire</i>	0.25	X	--	27,451
2	2016-11-01	<i>Proteus</i>	0.25	X	--	89,852
3	2016-11-01	USS <i>Tarpon</i>	0.25	X	--	106,293
4	2016-11-01	USS YP-389	0.35	X	--	157,729
5	2016-11-02	<i>Empire Thrush</i>	0.15	X	--	127,509
6	2016-11-02	U-701	0.25	X	--	47,609
7	2016-11-03	<i>Malchace</i>	0.35	X	--	204,357
8	2016-11-03	<i>Merak</i>	0.25	X	--	223,656
9	2016-11-05	HMS <i>Senateur Duhamel</i>	0.20	X	--	140,516
10	2016-11-06	<i>F.W. Abrams</i>	0.25	X	--	319,008
11	2016-11-06	USS <i>Monitor</i>	0.40	X	--	810,726
12	2017-07-05	<i>Ashkhabad</i>	0.25	X	X	95,953
13	2017-07-06	<i>W.E. Hutton</i>	0.35	X	X	233,401
14	2017-07-06	USS <i>Schurz</i>	0.25	X	X	179,837
15	2017-07-06	U-352	0.35	X	X	46,795
16	2017-07-10	<i>W.E. Hutton</i>	0.35	X	X	279,055
17	2017-07-11	<i>W.E. Hutton</i>	0.35	X	X	171,117
18	2017-07-12	USS <i>Schurz</i>	0.25	X	X	175,311
19	2017-07-13	HMT <i>Bedfordshire</i>	0.25	X	X	86,185
20	2017-07-14	U-352	0.35	X	X	62,225

**Table S3:** Representative species likely to be detected during fisheries acoustics surveys. This species list is from previous diver-conducted visual surveys on artificial and natural reefs on the continental shelf of North Carolina, USA (Paxton et al. 2017). The probability of detecting a species with fisheries acoustics is given as high for species with pelagic habitat associations and low for species with demersal habitat associations. Two species highlighted in bold are partially planktivorous species that predominantly consume zooplankton during life phases occupied at the sizes we commonly encounter them.

functional group	detection probability	habitat association	genus	species	common name		
planktivore	high	pelagic	<i>Decapterus</i>	<i>macarellus</i>	Mackerel Scad		
		pelagic	<i>Decapterus</i>	<i>punctatus</i>	Round Scad		
		pelagic	<i>Decapterus</i>	sp.	Decapterus Species		
		<b>pelagic</b>	<b><i>Haemulon</i></b>	<b><i>aurolineatum</i></b>	<b>Tomtate</b>		
		pelagic	<i>Menidia</i>	<i>menidia</i>	Silversides		
planktivore	low	<b>pelagic</b>	<b><i>Rhomboplites</i></b>	<b><i>aurorubens</i></b>	<b>Vermillion Snapper</b>		
		demersal	<i>Chromis</i>	<i>cyanea</i>	Blue chromis		
		demersal	<i>Chromis</i>	<i>enchrysur</i>	Yellowtail Reef Fish		
		demersal	<i>Chromis</i>	<i>scotti</i>	Purple Reef Fish		
		demersal	<i>Parablennius</i>	<i>marmoreus</i>	Seaweed Blenny		
piscivore	high	demersal	<i>Ptereleotris</i>	<i>calliura</i>	Blue dartfish		
		demersal	<i>Thalassoma</i>	<i>bifasciatum</i>	Bluehead wrasse		
		pelagic	<i>Carangoides</i>	<i>bartholoma</i>	Yellow Jack		
		pelagic	<i>Carcharias</i>	<i>taurus</i>	Sandtiger Shark		
		pelagic	<i>Euthynnus</i>	<i>alletteratus</i>	Little Tunny		
		pelagic	<i>Scomberomorus</i>	<i>cavalla</i>	King Mackerel		
		pelagic	<i>Scomberomorus</i>	<i>maculatus</i>	Spanish Mackerel		
		pelagic	<i>Seriola</i>	<i>dumerili</i>	Greater Amberjack		
		pelagic	<i>Seriola</i>	<i>fasciata</i>	Lesser Amberjack		
		pelagic	<i>Seriola</i>	<i>rivoliana</i>	Almaco Jack		
		pelagic	<i>Sphyraena</i>	<i>barracuda</i>	Barracuda		
		pelagic	<i>Sphyraena</i>	<i>borealis</i>	Northern Sennet		
		pelagic	<i>Sphyraena</i>	<i>guachancho</i>	Guaguanche		
		piscivore	low	demersal	<i>Ablennes</i>	<i>hians</i>	Flat Needlefish
				demersal	<i>Anguilliformes</i>	sp.	Unknown Eel
demersal	<i>Epinephelus</i>			<i>inermis</i>	Marbled Grouper		
demersal	<i>Mycteroperca</i>			<i>interstitialis</i>	Yellowmouth Grouper		
demersal	<i>Mycteroperca</i>			<i>phenax</i>	Scamp		
		demersal	<i>Pterois</i>	<i>volitans</i>	Lionfish		
		demersal	<i>Synodus</i>	<i>foetens</i>	Inshore Lizardfish		

**Supplement 2:** Detailed methods for quantifying fishes and zooplankton.

The SBES (SIMRAD EK60; 7° beam angle) emitted sound pulses downwards into the water at three frequencies: 38 kHz, 120 kHz, and 200 kHz to detect zooplankton, fishes, the shipwreck structure, and the surrounding seafloor on transect lines established around each shipwreck. For the 38- kHz frequency, the pulse length was 0.256  $\mu$ s, whereas for the 120- kHz and 200- kHz frequencies, the pulse length was 0.128  $\mu$ s. To reduce acoustic interference among sonar transducers, the SBES emitted pings when triggered by the MBES. As such, the ping rate for the SBES was determined by parameters set for the MBES. The SBES was calibrated using a tungsten carbide sphere to enable accurate measurements of fish size (Foote et al. 1987).

SBES data were processed with Echoview version 8.0 (Myriax Software Pty. Ltd 2017) to quantify the spatial distribution of zooplankton and fishes around each shipwreck. Data were corrected to account for the location of the transducers and the motion of the ship (pitch and roll), which was logged during data collection with the differential GPS and Applanix POS M/V motion sensor. We verified that the echosounder-detected bottom corresponding to the seafloor and shipwrecks was accurate; if the bottom had been assigned inaccurately, then it was manually corrected. Data beneath the corrected bottom-line were excluded from further analyses. To remove acoustic interference at the water surface created by bubbles, we excluded from the surface (0 m depth) down to 7.5 m beneath the surface. If the bubbles extended deeper than 7.5 m into the water column, then they were manually removed up to their deepest extent. Impulse noise from the ADCP was removed from SBES data using an algorithm that detected samples containing noise and then replaced those samples with the mean values from the surrounding samples (Ryan *et al.* 2015)(settings: vertical window = 5 samples, horizontal context window = 5 pings, sample threshold = 10 dB).

Individual fishes and schools of fishes were identified from the 120 kHz SBES data. Individual fishes were detected using a 2D fish tracking algorithm (Echoview 2017). We visually inspected the resulting fish tracks to verify that sequential single targets were identified correctly as either fish tracks or not. Metrics describing each individual fish track were exported for further analysis. For fishes occurring in schools, we applied the SHAPES algorithm (Barange 1994) separately to each school to delineate the boundaries of the school. We extracted two sets of data from the schools. First, we applied the algorithm using a minimum volume backscattering coefficient ( $S_v$ ) of -65 dB. The resulting schools were integrated to determine the volume backscattering strength of each school and position of the school, and these values were exported for further analysis. Second, we defined the perimeter of each school where fishes were visible as distinct targets. To select only the perimeter of the school, we applied the SHAPES algorithm with a minimum  $S_v$  of -40 dB corresponding to the strongest return signals in each school where fishes overlapped since they were densely aggregated. These densely aggregated fishes were masked from the school, leaving only those loosely-spaced and clearly-defined fishes in the perimeter of the schools. Fishes in the perimeter of the schools were then detected as single targets and exported for further analysis. To avoid double counting fishes in the perimeter of schools that were distinct individual fishes as both schooling fishes and as individual fishes, the loosely-aggregated fishes in the perimeter of the schools were included in schooling fish analyses but masked from individual fish analyses.

All fish data were exported from Echoview in cells measuring 5 m (horizontal) by 1 m (vertical, depth) and a threshold of -65 dB. For each cell, the approximate volume of water sampled ( $V_{cell}$ ) was calculated automatically within Echoview during data export in a two-step process (Kieser and Mulligan 1984). First, the volume sampled for one ping ( $V_{ping}$ ) was calculated as:

$$V_{ping} = \frac{l}{N} \sin \frac{\phi}{2} \sum_{i=0}^{n-1} \delta_i (R_{i+1}^2 - R_i^2) [m^3] \quad (S1)$$

where  $l$  is the length of the cell along the cruise track [m],  $N$  is the number of pings in the cell to be analyzed ( $N = 1$  for  $V_{ping}$ ),  $\phi$  is the across track beam angle,  $\delta$  is a parameter indicating data to be excluded from the calculation ( $\delta = 0$ ; e.g., sample below the bottom line, sample above the surface line, or sample includes no data or bad data) or otherwise included in the calculation ( $\delta = 1$ ), and  $R$  represent the range [m], measured along the beam axis, from the

start ( $R_i$ ) to the end ( $R_{i+1}$ ) of the analysis domain. Second, the volume sampled per ping ( $V_{ping}$ ) for the pings inside of each cell was summed to obtain the volume sampled per cell ( $V_{cell}$ ) as:

$$V_{cell} = \sum_{p=1}^N V_{ping} \quad [m^3] \quad (S2)$$

The resulting volume sampled per cell ( $V_{cell}$ ), known as the ‘wedge volume sampled,’ approximates the sampled volume of water. It is based on several assumptions: 1) distance traveled over the analysis domain (e.g., each cell) is a straight line and 2) speed of the survey vessel and ping rate are uniform. This approach for calculating the volume sampled accounts for time-varied gain and is appropriate for vessel speeds and/or ping rates that result in overlapping or non-overlapping pings (Kieser and Mulligan 1984). Because these volumes were used later to calculate the density of individual fishes, rather than schooling fish density or zooplankton backscatter, these volumes were calculated from the single target detection echogram that excluded portions of the cell categorized as wreck structure or seafloor, as well as portions of the cell classified as fish schools. This approach ensured that the calculated volume of the cell matched the actual volume in which individual fishes could be detected, providing correct density values.

Exported metrics for both individual fishes (e.g., outside of schools) and fish schools were processed with R, version 3.3.2 (R Core Team 2016) to calculate fish density per cell (5 m horizontal x 1 m vertical). For individual fishes, we divided the number of fish per cell ( $N_{fish}$ ) obtained from the tracked fishes by the approximate volume of water sampled per cell ( $V_{cell}$ ) obtained from the single target detection echogram to calculate the density of individual fishes (e.g., non-schooling) per cell ( $\rho_{volume (individual)}$ ) (Parker-Stetter *et al.* 2009):

$$\rho_{volume(individual)} = \frac{N_{fish}}{V_{cell}} \left[ \frac{fish}{m^3} \right] \quad (S3)$$

If the track of an individual fish spanned more than one cell, the fish was assigned to the cell where the endpoint of its track occurred.

For the entirety of each fish school (e.g., extent of each school over multiple cells), the mean target strength ( $TS$ ) of fish detected in the perimeter of the school was first converted from the logarithmic to linear form as the backscattering cross section ( $\sigma_{bs}$ ):

$$\sigma_{bs} = 10^{TS/10} \quad [m^2] \quad (S4)$$

Then, for each cell that included part of the school, the volume backscattering strength of each cell attributed to the school ( $S_v$ ) was converted from the logarithmic to linear form as the volume backscattering coefficient ( $s_v$ ):

$$s_v = 10^{S_v/10} \quad [m^{-1}] \quad (S5)$$

Lastly, the volume density of each school ( $\rho_{volume (school)}$ ) per cell was calculated by dividing the volume backscattering coefficient ( $s_v$ ) by the backscattering cross section ( $\sigma_{bs}$ ) corresponding to the particular school of fishes:

$$\rho_{volume(school)} = \frac{\sigma_{bs}}{s_v} \left[ \frac{fish}{m^3} \right] \quad (S6)$$

This approach assumed that when a school spanned multiple cells, all of the fishes in the school were the same species and thus had the same backscattering cross section ( $\sigma_{bs}$ ).

The volume density of each school and the volume density of the individual fishes were added together for each cell to calculate the total volume density of fishes per cell ( $\rho_{volume(total)}$ ) as:

$$\rho_{volume(total)} = \rho_{volume(school)} + \rho_{volume(individual)} \left[ \frac{fish}{m^3} \right] \quad (S7)$$

Total volume density of fishes was calculated for all fishes, as well as fishes corresponding to three size classes: small (< 11 cm fish length), medium (11-29 cm fish length), and large (>29 cm fish length). Size class assignments were based on the general logarithmic equation for the relationship between mean target strength ( $TS_{mean}$ ) and fish total length (Love 1977):

$$Fish_{length} = 10^{(TS_{mean}+64.0035)/19.2} [cm] \quad (S8)$$

For individual fishes, these assignments were based on the  $TS_{mean}$  of each individual fish. For schooling fishes, size class assignments were based on  $TS_{mean}$  of fishes in the perimeter of the entire school, again assuming each school was composed of fishes of the same size.

Zooplankton were identified from the SBES data using decibel differencing, a technique capable of distinguishing zooplankton from fishes by comparing the mean volume backscattering strength ( $S_v$ ) detected by echosounders operating at multiple discrete frequencies (Higginbottom *et al.* 2000; Korneliussen and Ona 2003). Decibel differencing was conducted in Echoview using data from the 38 kHz and 120 kHz transducers. Since the pulse lengths of the 38 kHz and 120 kHz differed (0.256  $\mu$ s and 0.128  $\mu$ s, respectively), the 120-kHz data were resampled by time using a mean function so that the resulting resampled 120-kHz data had a pulse length of 0.256  $\mu$ s, matching the pulse length of the 38-kHz transducer data. The resampled 120-kHz data and the original 38-kHz data were smoothed using a median statistic applied to 3 samples (rows) and 3 pings (columns). The 3- kHz echogram was subtracted from the 120-kHz echogram to visualize the zooplankton. Fishes characterized as individuals and schools were masked from the zooplankton echogram, preserving only the zooplankton. These exclusively zooplankton data were exported by cells from the 38-kHz echogram matching the dimensions of cells for the fishes (5 m intervals x 1 m layers) using a threshold of -65 dB. Within R (R Core Team 2016), the mean volume backscattering strength ( $S_v$ ) of zooplankton was converted from the logarithmic (dB re 1  $m^{-1}$ ) to linear form ( $m^{-1}$ ), as per fishes above, to generate the volume backscattering coefficient ( $s_v$ ) of zooplankton per cell.

Fully processed SBES data included a per cell value corresponding to the volume density of both total fishes and fishes separated by size classes (fish  $m^{-3}$ ), as well as the volume backscattering coefficient of zooplankton ( $m^{-1}$ ). We refer to the volume backscattering coefficient of zooplankton as the zooplankton concentration.

## Literature Cited

Barange, M. (1994) Acoustic identification, classification and structure of biological patchiness on the edge of the Agulhas Bank and its relation to frontal features. *South African Journal of Marine Science* 14, 333–347.

Echoview (2017) Fish tracking algorithm: Echoview's Alpha-Beta tracking algorithm. Available at:

[http://support.echoview.com/WebHelp/Reference/Algorithms/Fish\\_tracking\\_module/Fish\\_tracking\\_algorithms.htm](http://support.echoview.com/WebHelp/Reference/Algorithms/Fish_tracking_module/Fish_tracking_algorithms.htm) [Accessed July 20, 2009].

- Foote, K.G., Knudsen, H.P., Vestnes, G., MacLennan, D.N. and Simmonds, E.J. (1987) Calibration of acoustic instruments for fish density estimation: a practical guide. *ICES Cooperative Report* 144, 1–57.
- Higginbottom, I.R., Pauly, T.J. and Heatley, D.C. (2000) Virtual echograms for visualization and post-processing of multiple-frequency echosounder data. In: *Proceedings of the Fifth European Conference on Underwater Acoustics*, Vol. ECUA 2000. pp 1497–1502.
- Kieser, R. and Mulligan, T.J. (1984) Analysis of echo counting data: a model. *Canadian Journal of Fisheries and Aquatic Sciences* 41, 451–458.
- Korneliussen, R.J. and Ona, E. (2003) Synthetic echograms generated from the relative frequency response. *ICES Journal of Marine Science* 60, 636–640.
- Love, R.H. (1977) Target strength of an individual fish at any aspect. *The Journal of the Acoustical Society of America* 62, 1397–1403.
- Myriax Software Pty. Ltd (2017) Echoview, version 8.0. Myriax Software Pty. Ltd, Hobart, Australia.
- Parker-Stetter, S.L., Rudstam, L.G., Sullivan, P.J. and Warner, D.M. (2009) Standard operating procedures for fisheries acoustic surveys in the Great Lakes. Great Lakes Fish. Comm. Spec. Pub. 09-01.
- R Core Team (2016) R: A language and environment for statistical computing.
- Ryan, T.E., Downie, R.A., Kloser, R.J. and Keith, G. (2015) Reducing bias due to noise and attenuation in open-ocean echo integration data. *ICES* 72, 2482–2493.

**Supplement 3:** Detailed methods for quantifying water currents.

The hull-mounted ADCP (Teledyne RDI Ocean Surveyor 150 kHz) recorded the magnitude and direction of water currents in 2-m vertical bins above and around the shipwrecks. ADCP data were processed with the University of Hawaii DAS system (UHDAS) (Firing and Hummon 2010; Firing *et al.* 2012) to account for beam volume, geometry, transducer orientation, and heading using custom UHDAS Python (Python Software Foundation 2017) scripts. These scripts produced Matlab (The Mathworks Inc. 2017) files containing the corrected five-minute averaged velocity profiles for each 2-m vertical bin. Data were also edited manually within the UHDAS interface to remove outliers and bad data. Data were further processed in Matlab using a custom UHDAS script that calculated the velocity of the currents from the velocity of water relative to the ship, measured by the ADCP, and the velocity of the survey vessel, determined from the differential GPS and Applanix POS M/V data. The component of current velocity in the east-west direction above and around the wreck ( $u$ ) was calculated for each 2-m vertical bin as the sum of the velocity of the water measured by the ADCP ( $u_{measured}$ ) and the velocity of the survey ship ( $u_{ship}$ ):

$$u = u_{measured} + u_{ship} \left[ \frac{m}{s} \right] \quad (S1)$$

The north-south component of current velocity ( $v$ ) was calculated in the same manner. Bad data values, such as those containing noise, bubbles, ping interference, or bottom interference, were also removed using the same custom UHDAS script within Matlab.

For each survey, the processed ADCP data corresponding to the duration of the SBES surveys conducted above and around each wreck were used to calculate the mean current magnitude and direction in Matlab with three steps. First, the east-west velocities and north-

south velocities were each averaged across the entire water column and across the spatial extent of the ADCP survey to obtain the mean velocity components ( $U$  and  $V$ ) for each survey. Second, the current magnitude ( $|\vec{U}|$ ) was calculated from the east-west ( $U$ ) and north-south ( $V$ ) velocity components as:

$$|\vec{U}| = \sqrt{U^2 + V^2} \quad \left[ \frac{m}{s} \right] \quad (S2)$$

Third, the direction of the current ( $\theta$ ) was calculated in radians as the inverse tangent of the east-west ( $U$ ) and north-south mean ( $V$ ) velocity components:

$$\theta = \tan^{-1} \left( \frac{U}{V} \right) \quad [rad] \quad (S3)$$

Direction values in radians were converted to degrees clockwise from north.

#### Literature Cited

Firing, E. and Hummon, J.M. (2010) Shipboard ADCP measurements. The GO-SHIP repeat hydrography manual: a collection of expert reports and guidelines. IOCCP Report No. 14, ICPO Publication Series No. 134.

Firing, E., Hummon, J.M. and Chereskin, T.K. (2012) Improving the quality and accessibility of current profile measurements in the Southern Ocean. *Oceanography* 25, 164–165.

Python Software Foundation (2017) Python v. 2.7.12.

R Core Team (2016) R: A language and environment for statistical computing.

The Mathworks Inc. (2017) MATLAB v. 2017b.

#### Supplement 4: Detailed methods for data analyses.

Fish, zooplankton, and current data were analyzed in R. Per cell values of zooplankton concentration ( $m^{-1}$ ), small fish density (fish  $m^{-3}$ ), medium fish density (fish  $m^{-3}$ ), and large fish density (fish  $m^{-3}$ ) were each summed across the entire water column vertically. These resulting-depth-collapsed values for each organism (zooplankton area concentration ( $m^2$ ) and fish area density ( $m^2$ ) per size class) were used for spatial analyses. Here, we call ‘small fishes’ planktivorous fishes, and we call ‘medium fishes’ and ‘large fishes’ piscivorous fishes. We report medium fishes separately from large fishes because the two different size classes help distinguish between the ecological roles of these fishes. Analyses were conducted for each of the twenty surveys, unless otherwise noted. Many of the analyses included calculation of spatial indicators developed specifically for geostatistical data like our fisheries acoustics data (Woillez *et al.* 2007, 2009). These spatial indicators are applicable for data like ours that inherently contain autocorrelation, even when other types of spatial analyses are inapplicable (Woillez *et al.* 2007, 2009).

*Spatial Location:* To describe the general spatial location of zooplankton, small fishes, medium fishes, and large fishes around artificial structures, we calculated spatial indicators for each organism: 1) positive area, 2) microstructure, 3) mean center, and 4) dispersion. We calculated these indicators by applying equations provided by Woillez *et al.* (2007, 2009). Here, we present the definition of each indicator, as well as the formula used to calculate it, as presented in Woillez *et al.* (2007, 2009), which are the appropriate citations for the below text on the spatial indicators. After calculating each indicator, we tested differences in

indicators among organism groups (zooplankton, small fish, medium fish, large fish) using one-way analyses of variance (ANOVAs) followed by post-hoc Tukey HSD tests.

Positive area (PA), which is the area occupied by each organism not including locations with zero density, was calculated as the sum of the area of influence ( $s_i$ ) around where fish density ( $z_i$ ) at sample  $i$  exceeds 0 as:

$$PA = \sum_i s_i 1_{z_i > 0} [m^2] \quad (S1)$$

Because PA excludes locations with zero density, this spatial indicator represents the area of organism presence. To account for differing total areas among shipwreck surveys, we divided PA [ $m^2$ ] by survey-specific total area [ $m^2$ ]. This provided us with scaled values representing the percent of the total survey area occupied by PA. Microstructure index (MI) was calculated to describe fine-scale variability in organism distribution. MI ranges from 0 to 1, where 0 represents a well-structured and regular density surface, whereas 1 represents a highly irregular and poorly structured density surface (Woiillez *et al.* 2007, 2009). MI was calculated as the relative decrease in the transitive covariogram ( $g$ ) constructed between distance  $0$  and distance  $h_0$  that is the mean lag between samples:

$$MI = \frac{(g(0) - g(h_0))}{g(0)} [0,1] \quad (S2)$$

Two indicators, mean center, which is also called the center of gravity (CG), and dispersion around the mean center, which is also called inertia (I), were calculated to describe the center of each organism's distribution and the spread around the center, respectively (Woiillez *et al.* 2007, 2009). CG, which is defined as the weighted mean center of each organism's distribution, was calculated as:

$$CG = \frac{\sum_{i=1}^N x_i s_i z_i}{\sum_{i=1}^N s_i z_i} [coordinates] \quad (S3)$$

where  $z_i$  is the organism density at point  $x_i$ , and  $s_i$  is the area of influence;  $i$  represents the sample number. I, which is the dispersion around the mean center, was calculated as:

$$I = \frac{\sum_{i=1}^N (x_i - CG)^2 s_i z_i}{\sum_{i=1}^N s_i z_i} [m^2] \quad (S4)$$

To determine how the mean center of organisms was positioned relative to the shipwreck, we calculated the distance between the mean center and edge of the shipwreck with the 'gDistance' function in the 'rgeos' package (Bivand and Rundel 2017). We also calculated the distance of each sampling cell containing fishes to the nearest shipwreck edge.

To further understand organism distribution, we identified clusters of high density (hot-spots) and low density (cold-spots). Hot-spots and cold-spots were detected using the Getis-Ord  $G_i^*$  statistic (Getis and Ord 1992; Ord and Getis 1995):

$$G_i^*(d) = \frac{\sum_{j=1}^n w_{i,j}(d) x_j}{\sum_{j=1}^n x_j} \quad (S5)$$

for sample location ( $i$ ) based on neighbors ( $j$ ) within a search radius ( $d$ ) with corresponding weight matrix ( $w_{i,j}(d)$ ) based on  $k$ -nearest neighbors. Getis-Ord  $G_i^*$  values were calculated for variables of interest ( $x$ ), fish density by size class and zooplankton concentration, using the 'localG' function within the 'spdep' package (Bivand and Piras 2015). The resulting  $z$ -values, representing standard deviation, indicated whether hot-spots (positive  $z$ -value) or

cold-spots (negative  $z$ -value) were present. To determine whether the hot- and cold-spots were statistically significant, we used the criteria that a  $z$ -value between 1.96 and -1.96 corresponded to  $p$ -values  $> 0.05$ , so  $Z$ -values  $> 1.96$  and  $< -1.96$  indicate a statistically significant hot-spot or cold-spot. This relationship is based on the generalized one-to-one relationship between  $z$ - and  $p$ -values that is used within ArcGIS implementations of the function as an alternative to applying critical values for different sample sizes (Ord and Getis 1995; ESRI 2016). This alternative implementation was appropriate for our data because each of our surveys had a different sampling extent and associated sample size.

*Spatial Relationships:* We quantified spatial relationships between organism pairs (e.g., zooplankton and small fishes, small fishes and medium fishes, etc.) at both global and local scales. At the global scale, we calculated the global index of collocation (GIC) (Woiillez *et al.* 2007, 2009). For two organisms with densities  $z_1(x)$  and  $z_2(x)$  at point  $x$  with respective CGs and inertias ( $CG_1$  and  $I_1$ , and  $CG_2$  and  $I_2$ ), the GIC is:

$$GIC = 1 - \frac{\Delta CG^2}{\Delta CG^2 + I_1 + I_2} \quad (S6)$$

Where  $\Delta CG$  is the difference between the  $CG_1$  and  $CG_2$ . GIC values range from 0 to 1 with 1 representing coinciding CGs with positive inertia values and 0 representing the opposite, where each organism has a different CG and 0 inertia. Two organisms with identical CGs but different inertias would have a GIC of 1, so the GIC does not provide information on how organisms are arranged at a finer scale (e.g., concentric distributions, etc.) (Bez and Rivoirard 2000).

To complement global metrics, we calculated a metric describing spatial overlap at the local scale, called the co-occurrence. While the GIC compared organism distribution over the entire extent of each survey, the local metric assesses overlap at the level of each sample (e.g., 5 m x 1 m depth collapsed sample). The local metric, co-occurrence (CO), is the proportion of samples ( $l$ ) where both species 1 and species 2 co-occurred during the same survey (Saraux *et al.* 2014):

$$CO = \frac{l_{1,2}}{l_1 + l_2} [0,1] \quad (S7)$$

CO includes samples where either one or both species are present and excludes samples where both species are absent. Together, the GIC and CO values provide complementary means to interpret relationships between two organism groups that were appropriate for fisheries acoustics data like ours. We bootstrapped the GIC and CO results for each pair of organism groups for all twenty surveys to ensure that the mean overlap metrics across all twenty surveys approximated the mean distribution from 1,000 bootstrapped pulls conducted within the ‘bootstrap’ package (Tibshirani and Leisch 2017).

*Water Current:* To determine how water current magnitude affected the location of planktivorous fishes relative to each shipwreck, we first calculated the distance from the mean center of small fishes to the shipwreck edges. We also calculated distances from the mean center of medium and large fishes from shipwreck edges. The distances were calculated with the ‘gDistance’ function in the ‘rgeos’ package (Bivand and Rundel 2017). We did not calculate the distance between the center of small fishes and zooplankton because zooplankton were present throughout nearly 25% of surveyed areas, meaning that their mean center was biased by survey extent. We used linear regressions to investigate relationships between fish location and current magnitude. First, we regressed distances between the mean center of each fish size class and the nearest shipwreck edge against current magnitude. Second, because small fishes were unrelated to water current and given prior research

suggesting that predator-prey dynamics influence planktivorous fish aggregations (Holzman *et al.* 2005), we fit additional linear regressions investigating relationships between the distance of small fishes from wreck edges and predictor variables representing apparent predation risk. The predictor variables for apparent predation risk were the number of medium, large, and both medium and large fishes present within the shipwreck, designated as the manually delineated polygon corresponding to the shipwreck structure, and 5-m outward of the delineated shipwreck structure. We conducted assessments of fit by comparing observed distances of small fishes from edges to those of the estimated distribution.

To determine how water current direction influenced small fish density, we visualized the location of the mean center of small fishes relative to upstream and downstream portions of the shipwreck. We designated the upstream and downstream areas corresponding to each survey where current data were collected. To make the upstream versus downstream distinction, we drew the current vector associated with each survey so that it bisected the survey extent through the centroid of the wreck. We then drew a line perpendicular to the current vector. Surveyed areas on either side of the perpendicular line were then designated as ‘upstream’ or ‘downstream.’ For example, areas that the current hit first were ‘upstream,’ and those areas that the current would move to only after passing the wreck were ‘downstream.’ We also used the upstream versus downstream designations to determine whether each sampling cell that corresponded to a value of fish density was upstream or downstream. To do this, we calculated the bearing between the centroid of the shipwreck and the sampling cells. We compared this bearing to the bearings required to be in the upstream or downstream sections of the sampling extent (on either side of the line perpendicular to the current vector). Fishes that occurred within the upstream extent were categorized as upstream, and those in the downstream extent as downstream. We calculated the total number of small fishes located upstream and downstream on each survey. We used these data to fit beta regressions using the ‘betareg’ package (Cribari-Neto and Zeileis 2010) to examine whether the proportion of fishes located upstream or downstream was affected by current magnitude.

#### Literature Cited

- Bez, N. and Rivoirard, J. (2000) Future applications of CUFES: indices of collocation between populations. In: *Report of a workshop on the use of the Continuous Underway Fish Egg Sampler (CUFES) for mapping spawning habitats of pelagic fish.* (eds D.M.J. Checkley, J.R. Hunter, L. Motos and C.D. van der Lingen). GLOBEC Report No. 14, pp 48–52.
- Bez, N. and Rivoirard, J. (2001) Transitive geostatistics to characterise spatial aggregations with diffuse limits: An application on mackerel ichthyoplankton. *Fisheries Research* 50, 41–58.
- Bivand, R. and Piras, G. (2015) Comparing implementations of estimation methods for spatial econometrics. *Journal of Statistical Software* 63, 1–36.
- Bivand, R. and Rundel, C. (2017) rgeos: Interface to geometry engine - open source (‘GEOS’).
- Cribari-Neto, F. and Zeileis, A. (2010) Beta regression in R. *Journal of Statistical Software* 2 34, 1–24.
- ESRI (2016) ArcGIS. Redlands, California, USA. Environmental Systems Research Institute.
- Getis, A. and Ord, J.K. (1992) The analysis of spatial association by use of distance statistics. *Geographical Analysis* 24, 189–206.

- Holzman, R., Reidenbach, M.A., Monismith, S.G., Koseff, J.R. and Genin, A. (2005) Near-bottom depletion of zooplankton over a coral reef II: Relationships with zooplankton swimming ability. *Coral Reefs* 24, 87–94.
- Ord, J.K. and Getis, A. (1995) Local spatial autocorrelation statistics: distributional issues and an application. *Geographical Analysis* 27, 286–306.
- R Core Team (2016) R: A language and environment for statistical computing.
- Saraux, C., Fromentin, J.-M., Bigot, J.-L., et al. (2014) Spatial structure and distribution of small pelagic fish in the northwestern Mediterranean Sea. *PLoS ONE* 9, e111211.
- Tibshirani, R. and Leisch, F. (2017) bootstrap: functions for the book “An Introduction to the Bootstrap.”
- Wuillez, M., Poulard, J.-C., Rivoirard, J., Petitgas, P. and Bez, N. (2007) Indices for capturing spatial patterns and their evolution in time, with application to European hake (*Merluccius merluccius*) in the Bay of Biscay. *ICES Journal of Marine Science* 64, 537–550.
- Wuillez, M., Rivoirard, J. and Petitgas, P. (2009) Notes on survey-based spatial indicators for monitoring fish populations. *Aquatic Living Resources* 22, 155–164.